IC4406: a radio-infrared comparison

L. Cerrigone[1,2], J. Hora[1], G. Umana[2], C. Trigilio[2]

[1] Harvard-Smithsonian Center for Astrophysics, USA; [2] Istituto Nazionale AstroFisica, Italy

Abstract: IC 4406 is a large (about 100'' x 30'') southern bipolar planetary nebula, composed by two elongated lobes, extending from a bright central region, where there is evidence for the presence of a large torus of gas and dust.

In this poster we show new observations of this source performed with IRAC (Spitzer Space Telescope) and the Australia Telescope Compact Array. Although the possibility for faint extended emission to be missing in the radio maps cannot be ruled out, flux from the ionized gas appears to be concentrated in the bright central region. Comparing ATCA to IRAC images, it seems that, like in other planetary nebulae, ionized and neutral components spatially co-exist in IC 4406.

Introduction

IC4406 is a well studied southern planetary nebula. It has been imaged with several telescopes and at different wavelength ranges. It shows two H_2 lobes (Storey, 1984), orthogonal to the nebula's major axis and each 15'' away from the center. These peaks are approximately coincident with the two blobs observed in Hα+NII and OIII in Sahai et al 1991, interpreted as indicative of the presence of a dense equatorial torus of dust. CO maps (Sahai et al, 1991) show the presence of a collimated high velocity outflow in the polar direction. Hubble images in NII, Hα and OIII have revealed the existence of an intricate system of dark lane features (O'Dell et al, 2002), which led to the name of "*Retina Nebula*" for this object (see Fig.4D).

We have observed this source in the radio range to inspect the distribution of the ionized gas in its envelope and in the infrared to check for emission from the equatorial dust and molecular gas.

Observations and Data reduction

Radio observations were performed at the **A**ustralia **T**elescope **C**ompact **A**rray[1] on November 24, 2005 (UT: 17:00:00; 08:00:00) and December 11, 2005 (UT: 15:30:00, 02:00:00), simultaneously at 4.8 and 8.6 GHz.

The November run was performed with the array in *1.5C* configuration, while for the December one the configuration was *6.0A*. The adopted configurations are both linear but with different antenna positions, giving maximum baselines of 4500 m (1.5C) and 5939 m (6.0A), minimum baselines of 77 m (1.5C) and 337 m (6.0A). The pre-calibration of the array was performed observing 0823-500, while the absolute flux calibrator was 1934-638. Another target was also observed during our two runs and the total on-target time was about 7 hours for each of the two. The phase calibrator chosen for IC 4406 was 1431-48, which is 4.76° away from the target. The data were reduced with **MIRIAD**, following a standard reduction procedure as recommended in the MIRIAD User's Guide. The data from the two runs were combined into one dataset, obtaining a *uv* coverage from 0.9 to 96 kλ at 4.8 GHz and from 1.5 to 172 kλ at 8.6 GHz. These correspond to an angular resolution of 2.2'' at 4.8 GHz and 1.2'' at 8.6 GHz, while the largest observable structures (Largest Angular Scale) are 230'' and 140'' respectively. Tab.1 summarizes the results of our radio observations.

Infrared observations were performed with the **I**nfra**R**ed **A**rray **C**amera onboard **Spitzer Space Telescope** at 3.6, 4.5, 5.8 and 8.0 µm on March 06, 2004 (UT 09:54:16.311). Six High Dynamic Range 30 sec dithered frames were obtained at each wavelength, for a total exposure time of 180 sec per channel.

Basic Calibration Data were retrieved from Spitzer archive, cleaned to correct such artifacts as mux-bleeding and banding and then coadded using **IRACproc** (Schuster et al, 2006).

The whole nebula in each image was boxed with a polygon and the flux within such region was summed up. The same procedure was adopted for the field star observed West of the central core, so that its flux was subtracted to the overall nebula's one. The result was corrected for an infinite aperture, according to the IRAC Data Handbook and then converted into mJy (SST BCD files are in units of MJy/sr). Tab.2 shows the results of this procedure.

Results and Discussion

Our radio maps show the presence at 4.8 GHz of a 42'' x 56'' (3σ level) emitting region, elongated in E-W direction; at a 10% of the peak level the size of the emitting region is restricted to 32'' x 32''. At 8.6 GHz the 10% of the peak level gives a size of 36'' x 40'', in agreement with its 3σ level size.

The maps don't show any N-S blobs of emission. What is shown is a very intricate system of emitting lanes (Fig.2), which resembles what is observed by Hubble Space Telescope.

An inspection of the amplitude vs. *uv*-distance plots leads to the conclusion that faint extended emission may be missing in our radio maps despite the combination of an extended and a compact array configuration.

Fig.3 shows IRAC images of the central equatorial area of the nebula. They were plotted with a linear scale having the peak flux and 50% of it as thresholds. Channel 4 is clearly showing the emission from the torus of dust surrounding the central star. Its size is about 28'' x 20'', elongated in N-S direction and the angular distance between its peaks is about 14''. The overall size of the torus matches with the approximate size of the nebula in N-S (30''), although its peaks are much closer to the center than the H_2 blobs, which can indicate the torus is partly shielding the molecular gas from UV radiation.

Fig.4 is a combination of IRAC channels in linear scale (as in Fig.3 but with 0 as a minimum). Despite the lower resolution compared to Hubble images, IRAC is able to detect the faint emission from the neutral components in the envelope and reveals the structure of the elongated lobes. They show arches at different distances and inclinations from the central star, connected to the mass loss history. The arches which are angularly closer to the central star show larger blue emission. This implies they have higher temperature, which can be explained if they are intrinsically closer to the star. Arches' radii then appear to be larger in the polar direction than in the direction perpendicular to the sky, which corresponds to the idea of the central torus as a collimating agent.

Collecting literature data and adding our new measurements, we have built up the SED for our target from the radio to the near-IR. We have overplotted to the data the sum of the theoretical curves for free-free emission and blackbody radiation. Three blackbodies with different temperatures were used to match the infrared data. The curves were separately normalized to one point before being summed up to match the data points (Fig.5). As reported in Sahai et al (1991), more than one dust component is necessary to match the observations. Since fewer points were used in that study, a different number of components and different parameters were found. According to our calculations, cold, warm and hot dust need to coexist to explain current observations. Tab.4 reports some parameters calculated assuming two different distances as reported in the literature (Sahai et al, 1991, O'Dell et al, 2002).

We can speculate that in such a diversified dust environment further lower temperature components may exist and high sensitivity, high angular resolution observations with **ALMA** will sure give a fundamental contribution to understand the physics of circumstellar envelopes in planetary nebulae.

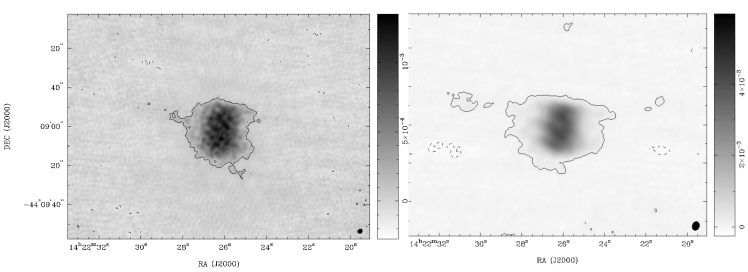

Fig.1: Radio maps of IC 4406 (*left*: 8.6 GHz; *right*: 4.8 GHz). The shown contours indicate ±3σ levels. Both maps were produced with NATURAL weights. The synthetic beam is shown in the bottom right of each map and the flux density unit is Jy/beam.

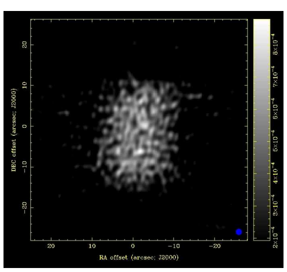

Fig.2: Zoom of 8.6 GHz map. The map was obtained with ROBUST weighting, to balance better resolution and sensitivity to faint structures. The RESTORed map was scaled to a 1.5'' beam, shown in bottom right. The flux density is in Jy/beam; the map is plotted with range from 3σ to peak value (linear scale).

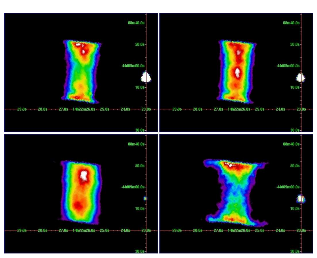

Fig.3 Zooms of the central core emission observed with IRAC. The scale is linear: maximum is the emission peak in the area, minimum is 50% of the maximum. Clockwise from top left: 3.6, 4.5, 5.8, 8.0 µm.

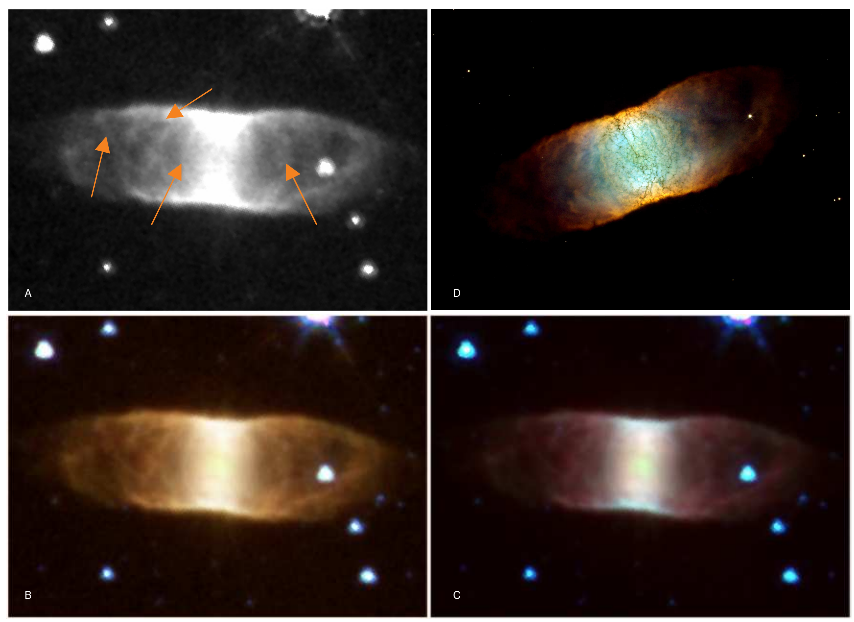

Fig.4: Counter-clockwise from top left. *A*: 5.8 µm image, scaled for a better view of the arches mentioned in the text, some of which are indicated by the arrows. *B*: overlay of IRAC channels. Blue is 3.6, Green 4.5, Orange 5.8 and Red 8.0 µm. *C*: as in B except that the 5.8 µm orange channel is not included. Here we can see the central torus emitting at longer wavelengths. *D*: Hubble image obtained combining Hα, NII and OIII emission (C. R. O'Dell et al, Hubble Heritage Team, NASA). In IRAC images N is up and E is left.

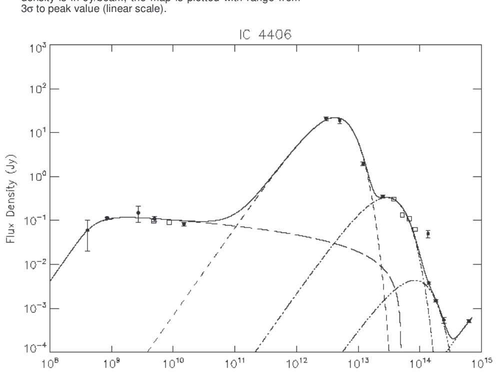

Fig.5: Spectral Energy Distribution with literature (solid circles) and new (open squares, with errors within each square) data. The single contributions are also plotted. Long dashed curve: free-free; dashed: blackbody at 72 K; dash-dot: blackbody at 490 K; dash-dot-dot: blackbody at 1400 K; dots: blackbody at 10^5 K.

	RA	DEC	4.8 GHz	8.6 GHz	σ
IC 4406	14:22:26.28	-44:09:00.0	96.47	91.15	0.04
1431-48	14:35:16.80	-48:21:47.76	1020	650	1

Tab.1: J2000 coordinates for our target and its phase calibrator, used for our ATCA run, are shown together with the observed flux densities and map noise (fluxes are in mJy).

	RA	DEC	3.6	4.5	5.8	8.0
IC 4406	14:22:27.66	-44:09:10.2	62.7	110.0	132.4	307.2

Tab.2: Pointing coordinates used for Spitzer Space Telescope observations. The estimated flux densities in each channel are shown in columns 4 through 6: units are mJy.

Distance (*kpc*)	0.7	1.6
$M_{ionized}$ ($M_\odot$)	0.11	0.88
M_{dust} ($M_\odot$)	$4.54 \cdot 10^{-5}$	$2.37 \cdot 10^{-4}$
M_D/M_{ion}	$4.06 \cdot 10^{-4}$	$2.68 \cdot 10^{-4}$
Density (cm^{-3})	$1.37 \cdot 10^3$	$0.90 \cdot 10^3$

Tab.4: Parameters calculated for two reported distances to our target. Density and ionized mass are calculated from 5 GHz data, according to Pottasch (1984), dust mass from 25 µm data, according to Pottasch et al (1984).

Radio		IRAS	IRAC	2MASS	Central Star
EM=$9.696 \cdot 10^5$	T=10000	T=72	T=490	T=1400	T=10^5

Tab.3: Parameters adopted to match observational points in Fig.4. Emission Measure is in cm^{-6}·pc, temperatures in *Kelvin*.

References

O'Dell, C.R., Balick, B., Hajian, A.R., Henney, W.J. and Burkert, A., 2002, AJ, 123, 3329
Pottasch, S., 1984, *Planetary Nebulae - A Study of Late Stages of Stellar Evolution*, D. Reidel Publishing Co.
Pottasch, S.R., Baud, B., Beintema, D., Emerson, J., Habing, H.J., Harris, S., Houck, J., Jennings, R. and Marsden, P., 1984, A&A, 138, 10
Sahai, R., Wooten, A., Schwarz, H.E. and Clegg, R.E.S., 1991, A&A, 251, 560
Schuster, M.T., Marengo, M. and Patten, B., 2006, SPIE, 6270, 65
Storey, J.W.V., 1984, MNRAS, 206, 521

Acknowledgements: L. Cerrigone acknowledges funding from the Smithsonian Astrophysical Observatory through the SAO Predoctoral Fellowship program. This work is based in part on observations made with the Spitzer Space Telescope, operated by Jet Propulsion Laboratory under NASA contract 1407.

[1] The Australia Telescope Compact Array is part of the Australia Telescope which is funded by the Commonwealth of Australia for operation as a National facility managed by CSIRO.